High-magnetic-field EPR in $Cd_{1-x}Mn_xTe$

L. M. Claessen*
Max-Planck-Institut für Festkörperforschung, Hochfeldmagnetlabor, Boîte Postale 166 X, F-38042 Grenoble CEDEX, France

A. Wittlin
Max-Planck-Institut für Festkörperforschung, Hochfeldmagnetlabor, Boîte Postale 166 X, F-38042 Grenoble CEDEX, France and Institute of Physics Al. Lotnikow 32/46 Pl-02668, Warsaw, Poland

P. Wyder
Max-Planck-Institut für Festkörperforschung, Hochfeldmagnetlabor, Boîte Postale 166 X, F-38042 Grenoble CEDEX, France
(Received 7 August 1989)

Magnetic resonances have been studied in $Cd_{1-x}Mn_xTe$ for $0.002 \leq x \leq 0.1$ by means of far-infrared magnetotransmission at fields up to $B = 22$ T. EPR of the Mn^{2+} ions is observed, accompanied by many orientation-dependent satellite resonances. These satellites are explained in terms of excitations of exchange-coupled Mn^{2+} pairs, and the presence of anisotropic exchange is strongly suggested. At $x \geq 0.02$ a very strong magnetic-field-induced line broadening is observed for $B > 10$ T. This broadening is explained in terms of a cross-correlation mechanism using exchange-coupled clusters as fast-relaxation centers.

I. INTRODUCTION

The low-temperature magnetic properties of the dilute magnetic semiconductor (DMS) $Cd_{1-x}Mn_xTe$ have recently been the subject of various experimental and theoretical investigations.[1-3] This wide-gap semiconductor is very well suited for the study of the whole variety of magnetic interactions as a function of Mn concentration. Up to approximately 70% of cadmium can be replaced by Mn ions while still preserving the fcc-zincblende lattice structure of CdTe. For very small concentrations ($x < 0.0001$) the magnetic ions are well separated in the nonmagnetic host lattice and EPR of single Mn^{2+} spins is observed.[14] For higher concentrations ($0.005 < x < 0.02$), interactions between neighboring spins become important. Dipolar interaction broadens the EPR spectrum, and exchange pairs of nearest neighbors (NN) are formed. The spin-glass-like phase has been reported[5] at low temperatures for $x > 0.2$. At concentrations $x > 0.6$ the crystal becomes antiferromagnetically ordered,[6] but it has been shown in several experiments that already at $x > 0.2$ short-range antiferromagnetic ordering is present.[7,8]

The origin of magnetic interactions between Mn^{2+} ions in wide-gap DMS has been recently studied both theoretically and experimentally. The localized character of 3D orbitals of manganese in these compounds and the absence of free carriers at low temperatures exclude long-range correlations of spins based either on the Ruderman-Kittel-Kasauya-Yosida (RKKY) mechanism or itinerant band interactions. While we still lack a detailed microscopic picture of the magnetic interaction, it is generally accepted that the basic mechanism is a superexchange-type antiferromagnetic correlation between the NN pairs of spins in the cation sublattice.[9,10] Also, next-nearest-neighbor (NNN) antiferromagnetic interactions, although about an order of magnitude weaker than NN exchange, seen to play an important role.[9-12] EPR techniques have been extensively used[13-18] to study the spin dynamics of paramagnetic DMS. However these studies have mostly been limited to the region of low fields ($B < 1$ T), where the external field was relatively weak compared to the internal exchange and dipole fields. On the other hand, magnetization measurements performed at fields up to 30 T indicated that in DMS, at these large fields, several different physical phenomena take place.[10,19]

In this paper we present the results of studies of magnetic interactions in $Cd_{1-x}Mn_xTe$ at high magnetic fields by means of high-field EPR spectroscopy. In these experiments, at far-infrared energies, low temperatures, and very high magnetic fields, EPR conditions are fundamentally different from those encountered in standard microwave spectrometers because of the fact that the thermal energy k_BT is considerably smaller than the electronic Zeeman energy splitting $g\mu B$. This means that only the lowest spin levels are populated and almost all spins are aligned along the external magnetic field. This external field may also be stronger than the internal dipole and exchange fields. Additionally, compared to low-frequency experiments, high-field EPR offers higher sensitivity,[20] which allows working with a simple transmission setup that, contrary to the microwave cavity technique, can be used over a broad frequency range.

A considerable experimental drawback in EPR at microwave energies is the presence of a significant linewidth increase upon temperature decrease or concentration increase,[14,17,18] which easily results in an experimental situation in which the broadening exceeds the resonance energy. This effect is still aggravated by the recently ob-

served shift of the resonance energy to lower magnetic fields for high concentrations.[8,14,16] Most EPR experiments done at microwave energies are therefore limited to either high temperatures or to low concentrations. The use of higher excitation energies (far-infrared) and consequently high-magnetic fields can overcome these drawbacks. Therefore in an earlier work[8] low-temperature EPR magnetotransmission experiments on high-concentration $Cd_{1-x}Mn_xTe$ were reported in the far-infrared region of the spectrum in high magnetic fields (up to 22 T). Very broad resonances (linewidths up to 10 T) were observed having a finite zero magnetic field energy and evolving with field as a $g=2$ resonance. These resonances have been explained in terms of single magnon excitation. In this paper we would like to extend these experiments to low-concentration $Cd_{1-x}Mn_xTe$, in which mostly single-spin EPR is observed, accompanied by small resonances coming from the excitation of nearest-neighbor exchange pairs. For Mn concentrations exceeding a few percent a dramatic magnetic-field-induced broadening of the EPR resonance line is also observed at fields above 10 T.

Already at low magnetic fields and relatively low Mn^{2+} concentrations ($0.002 < x < 0.05$), the EPR spectrum of $Cd_{1-x}Mn_xTe$,[21,22] as well as of analogous compounds,[23] contains besides the single Mn ion EPR contributions of exchange coupled NN and NNN pairs. Since these NN pairs are normally not excited at very low temperatures, because their ground state is the $S=0$ nonmagnetic singlet, one has to increase the temperature to populate higher spin states in order to observe the pair spectra. From the relative intensities of corresponding transitions one can then infer the magnitude of an exchange integral. Such a procedure has been excellently demonstrated for MgO:Mn and CaO:Mn by Harris.[23] On the other hand, as will be described later on, at fields at which the electronic Zeeman splitting becomes larger than the exchange energy J, a level crossing occurs[10,19,24] and the ground state becomes the $S=1$, $m=-1$ state of the triplet. This triplet state has a magnetic moment, and hence can be excited optically even at arbitrary low temperature. Therefore only at high-magnetic fields the pair magnetic transitions can be directly excited in such an EPR experiment. The level crossings at high fields, causing the change of the pair ground state from nonmagnetic to magnetic, have recently been observed[10,24] as steps in the sample magnetization at corresponding magnetic fields. In this paper we will show that at high fields the exchange pairs can be excited optically at low temperatures, and that their manifestation in the EPR spectra suggests the presence of anisotropic exchange.

II. EXPERIMENTAL

The single crystals of $Cd_{1-x}Mn_xTe$ with $0.002 \leq x \leq 0.1$ were grown by a modified Bridgeman technique at the Institute of Physics in Warsaw. The samples were cleaved along the $\langle 110 \rangle$ plane and polished in the form of slightly wedged disks of a few millimeters diameter and thickness between 0.4 and 4 mm.

Magneto-transmission measurements were made in the Faraday configuration at liquid-helium temperature, and for some samples also at temperatures up to 40 K. At fixed far-infrared frequencies, ranging in energy from one to a few meV, the transmission was monitored as a function of the magnetic field. The far-infrared (fir) radiation was generated by an optically pumped fir molecular gas laser. A standard lightpipe system was used to focus the radiation onto the sample. A liquid-helium-cooled carbon bolometer was used as a detector. To compensate for fluctuations in laser power during a magnetic field sweep, a similar detector was placed above the sample and both detector signals were divided after phase-sensitive detection in order to obtain the effective transmission of the sample. Superconducting coils (up to 13 T), and resistive Bitter magnets (up to 22 T) were used to generate magnetic fields. Special care was taken to avoid internal Fabry Perot interferences in the samples and standing wave phenomena in the lightpipes between laser, sample, and detector. Such phenomena are ubiquitous in far-infrared experiments, and in order to verify that the fine details of transmission spectra did not come from the experimental artifacts, the measurements have been repeated for varied sample shapes: from slightly wedged polished disks to roughly cut pieces. All measurements, also done at different arrangements of the laser-lightpipe system, reproduced the same spectral features. For the orientation dependent measurements the samples were aligned using an x-ray von Laue camera.

The aforementioned sensitivity of our measuring method is apparent in the transmission spectra. At the EPR resonance, the sample transmission drops even for thin low-concentration samples almost to the theoretical value of 50%, which is caused by a 100% absorption of the optically active circularly polarized component of the originally unpolarized fir radiation. Therefore, care must be taken to have sufficiently thin samples for linewidth determination in order not to saturate the resonance and consequently distort the line shape.

III. RESULTS

Figure 1 shows the low-temperature EPR spectra of samples with different Mn^{2+} concentration measured at

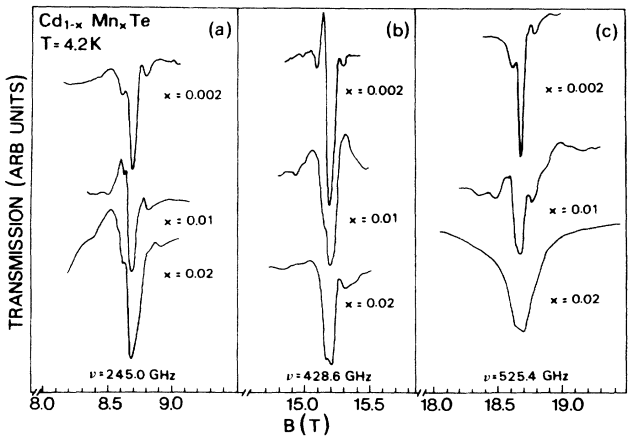

FIG. 1. The far-infrared transmission of several far-infrared frequencies for samples having different Mn^{2+} concentrations.

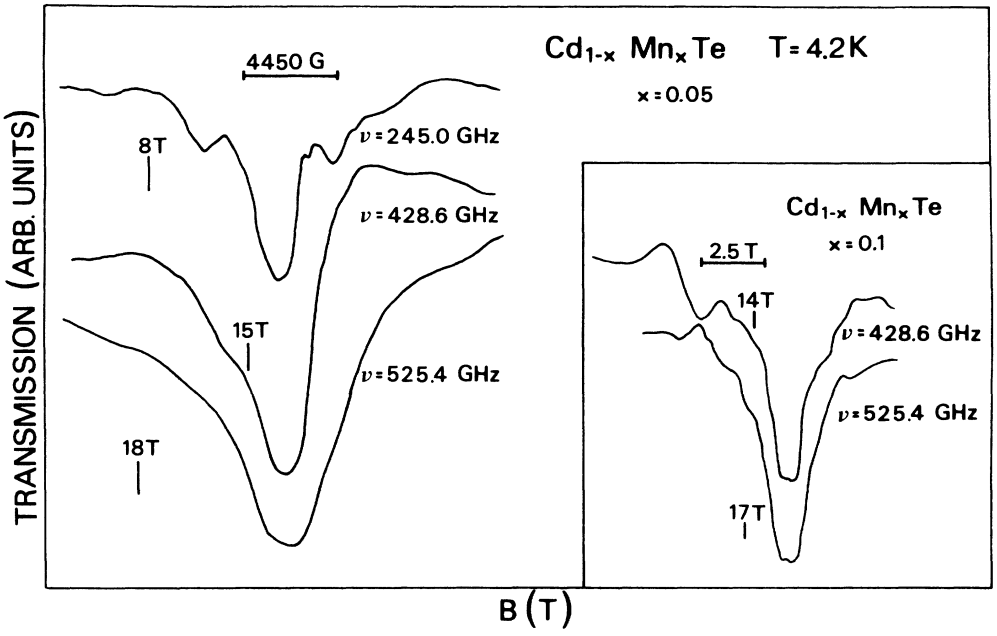

FIG. 2. The far-infrared transmission of a $x=0.05$ $Cd_{1-x}Mn_xTe$ sample showing the strong linewidth increase with field. In the inset two high-field spectra for a $x=0.1$ sample are shown.

245, 428.6, and 525.4 GHz. For all spectra the g factors corresponding to the main absorption peak equal 2.009 ± 0.003 (the accuracy is limited by the magnet calibration). At these low temperatures the resonance spectrum should consist of six closely spaced lines ($\simeq 50$ G) as a result of hyperfine interaction. Due to the limited resolution of our experiment, we would expect a single line of roughly 400 G linewidth, additionally broadened by the nuclear Zeeman effect (60 at 20 T). The full half power linewidth of the $x=0.002$ spectrum is, however, 600 ± 100 G. A similar broadening, which is only present at fields in excess of 5 T, has already been seen in much lower-concentration samples.[25,26] The reason of this broadening is unclear at present since the low manganese concentration seems to rule out all mechanisms concerning dipolar broadening[27,28] as possible causes. However, we can exclude line saturation noticing that the line shape remains unchanged over 2.5 orders of magnitude variations of laser power, and because the line shape was not dependent on sample thicknesses between a few mm and 200 μm. The linewidths for slightly higher concentrations ($x=0.01$ and 0.02) are bigger although for the fields below 10 T their values are in agreement with the low-frequency results. However, for the samples with $x\geq0.02$ we observe very strong broadening induced by the magnetic field. This effect is already noticeable in the $x=0.02$ sample above 10 T, and becomes more important in samples containing more manganese. Therefore, in Fig. 2, EPR spectra of a sample with $x=0.05$ are shown. In the inset of this figure two high-field EPR spectra of an $x=0.1$ sample are plotted to demonstrate the dramatic increase in linewidth with increasing concentration. To better display this effect, the linewidths as a function of field are shown for different Mn^{2+} concentrations in Fig. 3. The low-field values between brackets are values from other experiments.[2,16] These linewidths are defined by the transmission change of 50% compared to the transmission minimum. No attempts have been made to fit resonance lines by Lorentzian or Gaussian shapes because at high-fields standard descriptions of the EPR linewidths based on the second- and fourth-moment[27,29]

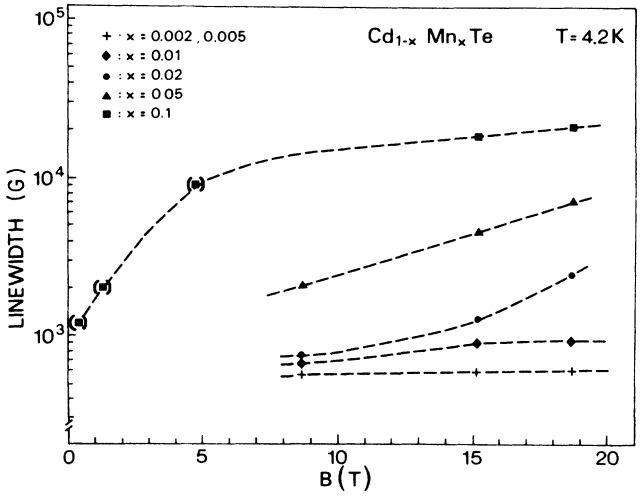

FIG. 3. The line width vs magnetic field as a function of Mn^{2+} concentration. The low-field values in brackets for the $x=0.1$ sample are literature values from other experiments. The dotted lines only serve as a guide to the eye.

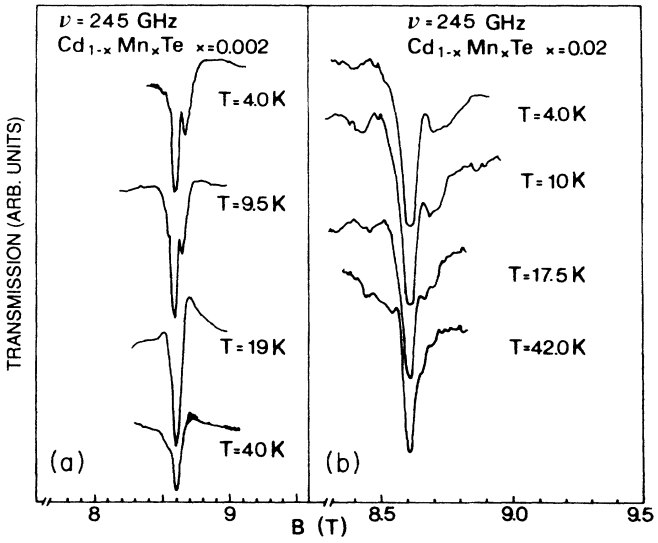

FIG. 4. The EPR spectra of the $x=0.002$ and $x=0.02$ samples for $\nu=245$ GHz for several temperatures.

analysis cease to be valid when[30] $g\mu B > k_B T$. Indeed as will be shown further on, the aforementioned extremely strong EPR line broadening at very high fields cannot be explained in the conventional way.

The salient feature of the spectra in Fig. 1 is the presence of many small satellite resonances around the main EPR peak. The position of these peaks relative to the main resonance seems to be rather independent on excitation energy although their relative strengths do depend on this energy.

To verify the temperature dependence, two samples of EPR spectra at 245 GHz were also recorded as a function of temperature and depicted in Fig. 4. It is clearly seen that the satellite line structure disappears at higher temperatures. The angular dependence of these satellites is shown in Fig. 5. In this figure a few spectra are shown of the $x=0.002$ sample at carefully oriented positions with respect to the magnetic field (the $\langle 110 \rangle$ respectively $\langle 100 \rangle$ crystal planes are oriented perpendicular to B). Although no orientation dependence on the position of the main EPR could be detected within the attainable accuracy of the experiment, indicating that the g factor must be highly isotropic, the positions of satellite lines strongly varies with the orientation. In Fig. 5(c) high-field spectra are shown for different sample geometries: respectively, a very thick (4 mm), $\langle 110 \rangle$-oriented single-crystal sample, and a compressed powder sample of the same thickness. The latter has no specific crystal orientation and shows only the main EPR resonance. The thick oriented sample shows in comparison with Fig. 5(b) the effect of sample thickness on the strength of the satellite

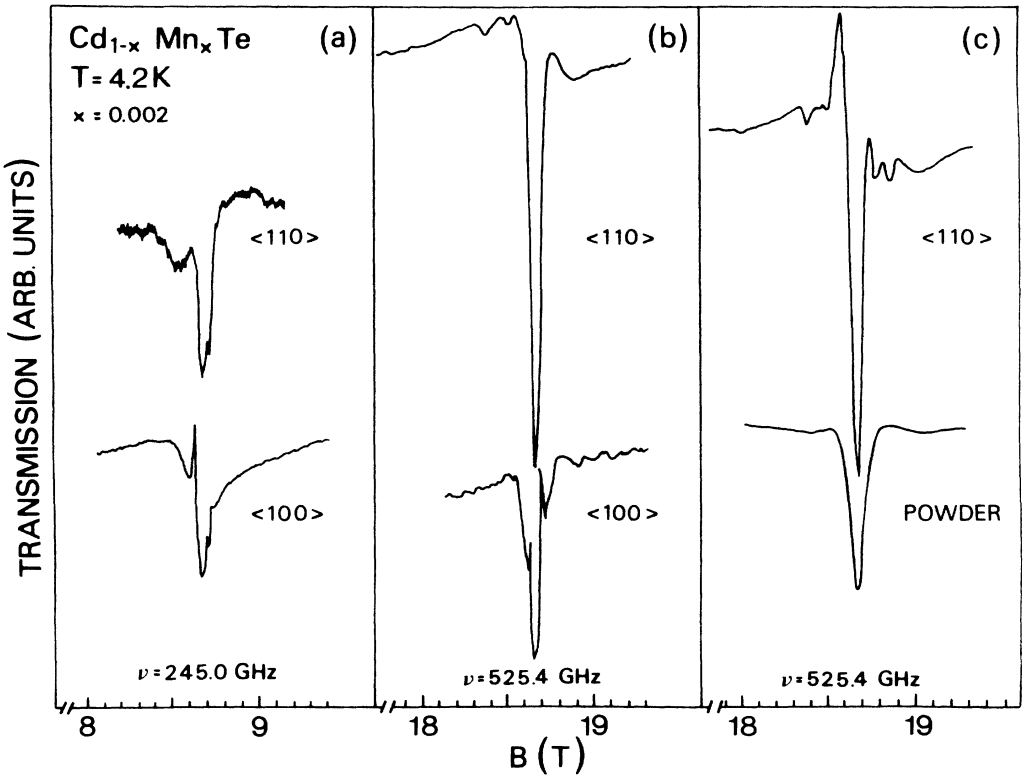

FIG. 5. The EPR spectra of the $x=0.002$ sample at several frequencies for the magnetic field oriented perpendicularly to respectively the $\langle 110 \rangle$ and the $\langle 100 \rangle$ crystal plane. (a) and (b) sample thickness 1 mm, and (c) sample thickness 4 mm and a 4-mm compressed powder sample.

lines relative to the main EPR line. Both these effects will be discussed more fully later on.

IV. DISCUSSION

The most apparent features of the high-field EPR spectra as shown in the previous section, e.g., the satellite lines and the strong broadening with field, are not observed at low-field EPR at low temperatures. As will be argued hereafter, these features can be attributed to the presence of exchange coupled spin pairs. The fundamental difference between high-field and low-field EPR is that at low fields and low temperatures all pairs reside in a nonmagnetic ground state and hence cannot be excited in an EPR experiment. Only at sufficiently high fields the ground state becomes a magnetic moment and contributes to the EPR spectra. We will now discuss how pair excitation can introduce satellite resonances around the main EPR line, as well as broadening at high fields. Moreover, it will be suggested that the presence of pair excitations at energies slightly different from the main EPR (e.g., satellite resonances) indicates the presence of anisotropic exchange.

Exchange pairs in DMS have already been observed by several groups in magnetization measurements,[10,19,24] in EPR,[21] and, more recently, in Raman scattering experiments.[22] From these experiments it is found that the concentration of pairs corresponds to their statistical distribution. Accordingly, the satellite resonances are EPR of NN exchange-coupled spin pairs. The energies of these transitions depend on an external field in the usual way, however, they slightly deviate from a $g=2$ single spin resonance due to the presence of anisotropic exchange. The importance of such an anisotropic exchange for EPR analysis in $Cd_{1-x}Mn_xTe$ has already been postulated by Ishikawa[12] in 1966, and can also be assumed per analogiam with results of Harris[23] for MgO:Mn. Moreover, in their recent analysis of EPR line shapes in $Cd_{1-x}Mn_xTe$, Samarth and Furdyna[16] suggested the Dzialoszynski-Moryia (DM) -type spin-spin interaction to be responsible for anisotropic exchange and their results have been quantitatively confirmed by calculations of Larson and Ehrenreich.[31] In this section we shall first discuss the pair spectra at high magnetic fields assuming anisotropic exchange, and then the influence of exchange pairs on the EPR lineshapes at high fields.

A. Pair spectra

In general, the spectrum of a Mn-Mn nearest-neighbor pair will consist because of hyperfine interactions of many lines with complicated angular dependence. A full analysis of such a spectrum would require a measurement accuracy, which is at present beyond the experimental possibilities of the high-magnetic-field setup. Therefore, by necessity, we have to limit our analysis to the most general features of a pair spectrum. Already at a concentration $x=0.002$, approximately 2% of the Mn^{2+} ions in $Cd_{1-x}Mn_xTe$ form pairs. Such a pair can be described in terms of two electronic spins $S=\frac{5}{2}$ according to the following spin Hamiltonian:[23,32,33]

$$\mathbf{H}=g\mu\mathbf{B}\cdot(\mathbf{S}_1+\mathbf{S}_2)+J\mathbf{S}_1\cdot\mathbf{S}_2+D_c\sum_{i=1}^{2}[S_{iz}^2-\tfrac{1}{3}S_i(S_i+1)]$$
$$+E_c\sum_{i=1}^{2}(S_{ix}^2-S_{iy}^2)+D_e(3S_{1z}S_{2z}-\mathbf{S}_1\cdot\mathbf{S}_2)$$
$$+E_e(S_{1x}+S_{2x}-S_{1y}S_{2y}) \quad (1)$$

in which all terms concerning hyperfine interaction have been omitted. The z axis is in the line joining two NN spins, which is in a $\langle 110\rangle$ crystal direction, and the x axis is in the direction of the Te ion of the Mn-Te-Mn ligand.[21] The y axis is consequently chosen to form an orthogonal right-handed coordinate system. g is the gyromagnetic factor, which equals 2, and μ is the Bohr magneton. J is the isotropic exchange interaction. The D_c and E_c terms present the distortion of the octahedral symmetry around each single spin, and the E_e and D_e terms present the anisotropic parts of the exchange term. The dipole-dipole interaction enters[12] as $-g^2\mu^2/r_{12}^3$ in D_e, which amounts to 2.25×10^{-3} meV for Mn^{2+} in CdTe for which the NN spin-spin separation equals 0.457 nm. Neglecting all anisotropic contributions, the isotropic exchange term J couples the spins to give pairs with a total spin S, which follow a Landé energy interval:

$$E_S=g\mu\mathbf{B}\cdot\mathbf{S}+\tfrac{1}{2}J[S(S+1)-\tfrac{35}{2}] \quad (2)$$

in which $S=0$, 1, 2, 3, 4, 5, and S_z takes values M from $-S$ to S. As in single spin EPR, optical transitions with $\Delta S=0$, $\Delta M=\pm1$ are allowed. In Fig. 6 the Landé energy interval is presented for Mn^{2+} pairs as a function of the magnetic field. J corresponds[10] roughly to a thermal

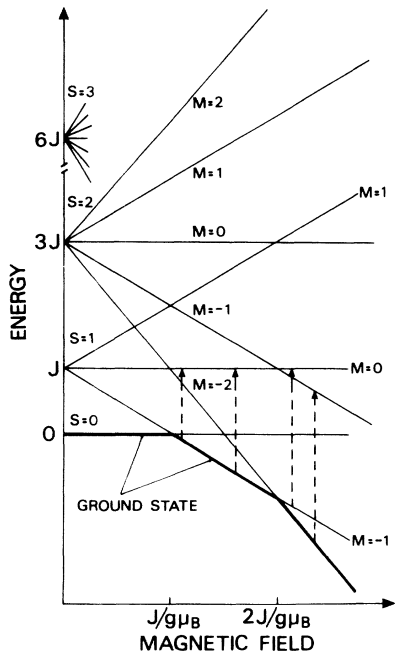

FIG. 6. The Lande energy interval for an exchange coupled pair of $S=\frac{5}{2}$ spins, and the evolution of the levels with magnetic field. In this plot $J/g\mu$ corresponds to about 9 T. The arrows suggest some allowed optical transitions. The heavy line indicates the ground state as a function of field.

energy of 10 K. The arrows correspond to allowed optical transitions. The heavy line corresponds to the populated ground state at zero temperature, and the absence of optical transitions at low temperatures and low-magnetic field is evident. Only at magnetic fields in excess of $J/g\mu(\simeq 9$ T),[34] the $S=1$, $M=-1$ state is populated due to the level crossing, and transitions to $S=1$, $M=0$ are possible. In this simplified isotropic picture however, these pair transitions are indiscernible from single spin EPR because the energy is the same. Including anisotropy terms from Eq. (1), and neglecting all terms of order $D^2/J, E^2/J$, the Hamiltonian can be rewritten as

$$g\mu\mathbf{B}\cdot\mathbf{S}+\tfrac{1}{2}J[S(S+1)-\tfrac{35}{2}]+D_s[S_z^2-\tfrac{1}{3}S(S+1)]+E_s(S_x^2-S_y^2) \tag{3}$$

with

$$D_s=3\alpha D_e+\beta D_c,\ E_s=\alpha E_e+\beta E_c\ ,$$

and

$$\alpha=\tfrac{1}{2}\frac{[S(S+1)+35]}{[(2S-1)(2S+3)]},\ \beta=\frac{[3S(S+1)-38]}{[(2S-1)(2S+3)]}\ ,$$

in which the E_s terms present the axial asymmetry with respect to the $\langle 110\rangle$ axis. The Hamiltonian from expression 3 is applicable to an arbitrary direction of the external magnetic field B in the coordinate system defined by the NN pair. For practical reasons this expression must be transformed to the laboratory frame in which we choose the external B field along the laboratory z axis. A spherical transformation of coordinates[35] yields for each spin pair the following expression:

$$\begin{aligned}\mathbf{H}=&g\mu BS_z+\tfrac{1}{2}J[S(S+1)-\tfrac{35}{2}]+D_s\{[\tfrac{3}{2}\cos^2(\theta)-\tfrac{1}{2}][S_z^2-\tfrac{1}{3}S(S+1)]\}\\&+E_s\{[\sin^2(\phi)-\cos^2(\phi)][\tfrac{3}{2}\cos^2(\theta)-\tfrac{3}{2}][S_z^2-\tfrac{1}{3}S(S+1)]\}\end{aligned} \tag{4}$$

in which θ and ϕ are the spherical coordinates of B in the pair coordinate system x,y,z, with θ the angle between B and z, and ϕ the angle between the projection of B on the x,y plane and the x axis. In obtaining Eq. (4) all terms giving rise to off-diagonal terms in the Hamiltonian have been neglected because $D_s, E_s \ll g\mu B, J$, and hence first-order perturbation theory is sufficient to obtain energy shifts due to anisotropy. We would like to stress the point that at very low magnetic fields this approach is not valid, and the Hamiltonian from Eq. (1) should be diagonalized. If in Eq. (4) axial symmetry is assumed, $E_s=0$ and the equation reduces to the expression given by Ishikawa[12] to describe the anisotropic interaction between Mn^{2+} ions in ZnS and CdS. From Eq. (4) it is derived that the excitation of a pair from state $S, S_z=M$ to $M+1$ will be seen in the transmission experiment as a resonance at a magnetic field H given by

$$\begin{aligned}H=&H_{\mathrm{EPR}}-\frac{1}{g\mu}D_s[\tfrac{3}{2}\cos^2(\theta)-\tfrac{1}{2}](2M+1)\\&-\frac{1}{g\mu}E_s[\sin^2(\phi)-\cos^2(\phi)][\tfrac{3}{2}\cos^2(\theta)-\tfrac{3}{2}](2M+1)\end{aligned} \tag{5}$$

in which H_{EPR} is the magnetic field at which the $g=2$ EPR resonance is observed. If the anisotropy is only of dipolar origin as already mentioned, then $H-H_{\mathrm{EPR}}=195$ G for $\theta=0$. To describe the transmission of a powder sample in which all orientations are equally present, the expression in Eq. (5) should be averaged over all angles θ and ϕ yielding

$$H=H_{\mathrm{EPR}}+\frac{1}{3g\mu}E_s(2M+1)\ . \tag{6}$$

Equations (5) and (6) should principally allow the determination of the anisotropy parameters D_c, D_e, E_e, and E_c. However, as already mentioned, accurate determination of these parameters is beyond the scope of this experiment. Moreover, Harris[23] has pointed out that due to exchange-striction and quadratic exchange effects the pair energies can differ considerably from the Landé interval given in Eq. (2). However, by estimating the strength of each transition from its abundance for each orientation together with a Boltzman distribution of the different S states as a function of the magnetic field, Eqs. (5) and (6) allow a semiquantitative simulation of the pair spectra showing its dependence on field and orientation.

In Fig. 5(c) an EPR spectrum of a powder sample is shown. The increased linewidth of the resonance compared to the spectra obtained from single crystals is due to averaging over many weak pair resonances near to the main EPR. A part of these resonances due to axial asymetry should not average out according to Eq. (6). Experimentally, however, only a single resonance line is observed within the attainable resolution, indicating that the total asymetry term E_s for low S must be smaller than the values deduced from previous investigations.[21] From Eq. (3) the term E_s consisting of a linear combination of E_c and E_e can be chosen in such a way as to vanish almost completely for low S. Using this constraint on E_c and E_e some simulations of low- and high-field spectra for the $\langle 110\rangle$ and the $\langle 100\rangle$ orientation are made and

shown in Fig. 7. The parameters used are $D_c = 4.2 \times 10^{-3}$ meV, $D_e = 2.1 \times 10^{-3}$ meV, $E_c = 7 \times 10^{-4}$ meV, and $E_e = 1.2 \times 10^{-3}$ meV, in which the absolute values of the E terms are not so stringent because effectively $E_s \ll D_s$ as already discussed. Each calculated resonance has been given a Lorentzian line shape to comply better with the experimental curves. Figure 7 shows a qualitative agreement with the experiment and predicts the trend as a function of both orientation and field. The simulations shown in this figure only serve as an order of magnitude estimation for the various anisotropy parameters. To our knowledge there are only very few experimental determinations of these parameters. The work of Wilamowski[21] on EPR of Mn-Mn pairs in $Cd_{1-x}Mn_xTe$ at microwave energies and higher temperatures distracts out of the hyperfine structure the following values: $D_c = -6.2 \times 10^{-3}$ meV, $D_e = 3 \times 10^{-3}$ meV, $E_c = -7.5 \times 10^{-4}$ meV, and $E_e = 2.23 \times 10^{-3}$ meV, which are close to values of Mn^{2+} in MgO by Harris,[23] and in a qualitative agreement with our results. The recently theoretically derived anisotropy values for D_1 starting from a DM type of interaction by Larson[31] *et al.*, also yield values of the same magnitude as our experiment.

It might be argued that in the low-concentration sample ($x = 0.002$) the presence of a few percent[10] of pairs should only give very weak intensity of pair resonances compared to the main EPR peak. However, as mentioned in a previous section, due to the sensitive measurement method the main EPR resonance always drops to nearly 50% transmission for samples thicker than ca. 0.5 mm, due to the onset of saturation. Therefore, a thicker sample did not cause the main EPR peak to become more prominent (although as previously mentioned, very thick samples showed some saturation broadening), but the weak satellites do become in such a case more pronounced relative to the main peak. This is shown experimentally in Figs. 5(b) and 5(c), in which the only difference between both ⟨110⟩-oriented spectra is a factor 4 in sample thickness.

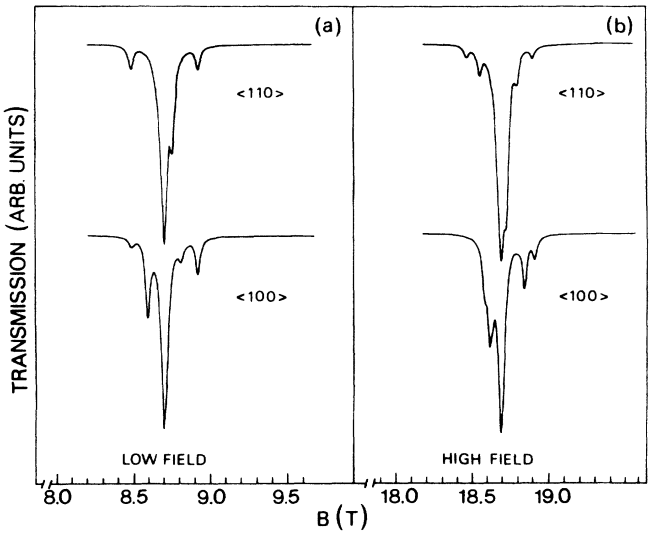

FIG. 7. Some theoretical transmission simulations of the pair excitations showing the dependence on magnetic field and crystal orientation. See the text for details.

In Fig. 4 it is shown that at temperatures $T > 10$ K the satellite lines are not observed anymore. In the experimental situation of the variable temperature measurement, this temperature corresponded to a thermal energy in excess of the electronic Zeeman splitting. The pair states which at low temperature were all in one triplet state will be thermally repopulated over several pair multiplets (see the Landé interval in Fig. 6), which all have [according to Eq. (4) and Eq. (5)] a different anisotropy energy. Hence the few lines from one triplet will be split up in many weak closely separated lines from various multiplets which results in a spectrum that cannot be resolved anymore with our experimental technique.

B. Broadening

In general EPR broadening mechanisms can be divided in static and dynamic mechanisms. The former incorporates mainly mechanisms related to additional internal field such as for instance dipolar broadening[27] or Dzialoszynski-Moryia (DM) anisotropy.[31] Dynamic effects exists mainly of lifetime broadening[36] due to very fast relaxation from the excited state. In the following, it will be argued that the usual static broadening effects are not likely to be responsible for the observed very strong broadening, and that dynamic effects might be important.

It has been suggested[13] that the main mechanism for the magnetic field induced broadening was an originally dipolar broadened but exchange narrowed resonance line at low fields. At high magnetic fields the EPR frequency attains the same order of magnitude as the exchange interaction frequency ($J/\hbar \simeq 5$ T), and the exchange narrowing becomes less effective.[29] Consequently, a line width increase should occur at high fields. However, even standard linewidth calculations discarding all possible narrowing mechanisms show that in the low-concentration DMS samples studied in this paper, already in the low-field limit any line broadening in excess of a few hundred Gauss cannot be due to dipolar effects.[27,28] Another mechanism recently evoked to explain the additional broadening in low-field EPR as observed[16] by Samarth *et al.* is the Dzialoszynski-Moryia type spin-spin interaction,[16,31] which has also been mentioned by the same authors as being a possible cause for the presence of anisotropic exchange. However, both above-mentioned broadening mechanisms cannot account for the very large scale broadening as observed in our experiments at high fields. Therefore, we like now to discuss the problem of lifetime broadening.

For isolated spins, spin relaxation (SRL) to the lattice normally goes by phonon interaction. The associated relaxation times for these processes are known to be very long at low temperatures[37,38] (up to 100 msec). Theoretically, this can be accounted for by the Blume-Orbach (BO) theory[39] on grounds of the fact that Mn^{2+} has no orbital momentum through which SRL goes most effectively. A second relaxation path for the spins as re-

cently noted[37,38] by Scalbert *et al.* is cross relaxation[32,36,40] through small clusters or pairs of Mn^{2+} which can play the role of fast relaxation centers. In Fig. 8 the different spin states with their relaxation rates are depicted to show the mechanism of cross relaxation. For low magnetic impurity concentrations (a few percent) the spin-spin relaxation time τ_{ss} is found to be much shorter[37] than the exchange-pair lattice relaxation time τ_{sl}. This τ_{sl} is usually much shorter than single spin lattice relaxation, due to the fact that lattice relaxation by phonon emission is much more effective for pairs than for singles. Moreover τ_{sl} decreases rapidly with increasing impurity concentration. In such a way the relaxation to the lattice through pairs or clusters can open up a very effective "by-pass" to relax, in which the experimentally important relaxation time in EPR (Ref. 41) is τ_{ss}. Unfortunately, there are not many direct experimental data available on τ_{ss} for $Cd_{1-x}Mn_xTe$. However, an extrapolation of the experimental data on τ_{sl} from Scalbert *et al.*[37] to higher concentrations, assuming $\tau_{ss} \ll \tau_{sl}$, suggests the presence of a very fast Zeeman-exchange relaxation not excluding subnanosecond values for τ_{ss}.

The reason that the above-discussed mechanism of cross relaxation is only effective at high magnetic fields can be understood by considering that at low temperatures the number of pair states with nonzero spin is very small in weak magnetic fields, but increases rapidly at magnetic field above 10 T due to the crossing[10] of the pair energy levels as discussed before (see also Fig. 6). Now spin-spin relaxation from single spins to pairs and clusters (the τ_{ss} channel of Fig. 8) becomes possible, making the effective excited spin lifetime very short. Also cluster forming through NNN exchange interaction is expected to contribute to this relaxation mechanism. Figure 3, which shows line widths versus magnetic field for several Mn concentrations indeed confirms that below 1% of Mn, where the fraction of pairs is low and the average distance between pairs and single spins large, the line width depends only very weakly on the field. On the other hand, a dramatic increase of the line width for 2% sample is observed above approximately 10 T which is about the field corresponding to the $S=0$, $S=1$ spin level crossing.

For larger x the line broadening starts already at lower fields and the linewidth increases monotonically with the field. For the 10% sample this linewidth tends to saturate above approx. 18 T. At these concentrations, although there are still a considerable fraction of pairs, the major contribution[10] will come from small clusters like triads, fourths, etc. At concentrations $x \geq 0.1$ the actual relaxation mechanism becomes extremely complicated because there can already exist an onset of short-range magnetic ordering. Indeed, Novak[7] *et al.* have shown the beginning of a spin-glass phase already at comparable low Mn^{2+} concentrations. An extension of the above-discussed mechanisms for relaxation might also be partially responsible for the extremely broad resonances seen[8] in high concentration AF ordered $Cd_{1-x}Mn_xTe$.

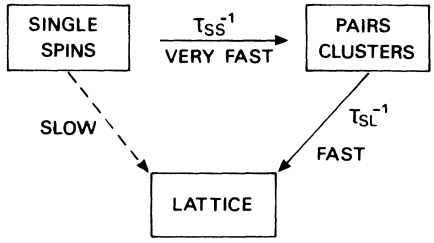

FIG. 8. The system with single spins, clusters, lattice, and relaxation rates showing the principle of cross relaxation.

Lately it has been argued[37] that the DM anisotropic exchange interaction, used to explain the EPR broadening[16] of low-concentration samples also plays a role in the relaxation mechanism in the clusters. At present there is however to our knowledge no experimental evidence for this.

V. CONCLUSIONS

We have measured EPR in low- and medium-concentration $Cd_{1-x}Mn_xTe$ at high magnetic fields and at far-infrared energies. The most important experimental results are the observation of orientation dependent satellite resonances around the main EPR resonance, and the presence of a strong magnetic field induced broadening. The presence of satellite resonances around the main EPR is due to excitation of exchange-coupled pairs of NN spins, and indicates the presence of anisotropic exchange. The estimations of the order of magnitude of the anisotropic exchange as deduced from the experiment comply well with the few available literature data. The strong magnetic field induced line broadening observed at fields above 10 T for $x > 0.01$ can be qualitatively explained by lifetime broadening due to cross relaxation, in which exchange coupled clusters play the role of vast relaxation centers. This mechanism only functions at high magnetic fields, because at low magnetic fields and low temperature these clusters reside in a nonmagnetic ground state.

ACKNOWLEDGMENTS

We would like to thank Professor Ludwig Genzel and Professor Henryk Szymczak for their interest in this work. We thank Dr. Z. Wilamowski for helpful discussion and showing us his results prior to publication. We also thank Professor R. R. Galazka and Dr. A. Mycielski for $Cd_{1-x}Mn_xTe$ samples. A. W. acknowledges financial support from the Max-Planck-Gesellschaft and the Polish Academy of Sciences (research project No. RPB 01.9).

*Present address: Philips Research Laboratories, P.O. Box 80000, 5600 JA Eindhoven, The Netherlands.

[1]W. Giriat and J. K. Furdyna, in *Semiconductors and Semimetals,* edited by J. K. Furdyna and J. Kossut (Academic, New York, 1988), Vol. 25, p. 1.

[2]S. Oseroff and P. H. Keesom, in *Semiconductors and Semimetals,* Ref. 1, p. 73.

[3]*Diluted Magnetic (Semimagnetic) Semiconductors,* Materials Research Society Symposium Proceedings, edited by R. L. Aggarwal, J. K. Furdyna, and S. Von Molnar (Materials Research Society, Pittsburgh, 1987), Vol. 89.

[4]J. Lambe and C. Kikuchi, Phys. Rev. **119**, 1256 (1960).

[5]R. R. Galazka, S. Nagata, and P. H. Keesom, Phys. Rev. B **22**, 3344 (1980).

[6]T. Giebultowicz and T. M. Holden, in *Semiconductors and Semimetals,* Ref. 1, p. 125.

[7]M. A. Novak, O. G. Symko, D. J. Zheng, and S. Oseroff, Phys. Rev. B **33**, 6391 (1986).

[8]A. Wittlin, L. M. Claessen, and P. Wyder, Phys. Rev. B **37**, 2258 (1988).

[9]A. Lewicki, J. Spalek, J. K. Furdyna, and R. R. Galazka, Phys. Rev. B **37**, 1860 (1988).

[10]B. E. Larson, K. C. Hass, and R. L. Aggarwal, Phys. Rev. B **33**, 1789 (1986).

[11]J. Spalek, A. Lewicki, Z. Tarnawski, J. K. Furdyna, R. R. Galazka, and Z. Obuszko, Phys. Rev. B **33**, 3407 (1986).

[12]Y. Ishikawa, J. Phys. Soc. Jpn. **21**, 1473 (1966).

[13]S. Oseroff, Phys. Rev. B **25**, 6548 (1982).

[14]R. E. Kremer and J. K. Furdyna, Phys. Rev. B **31**, 1 (1985).

[15]H. A. Sayad and S. M. Bhagat, Phys. Rev. B **31**, 591 (1985).

[16]N. Samarth and J. K. Furdyna, Phys. Rev. B **37**, 9227 (1988).

[17]D. J. Webb, S. M. Bhagat, and J. K. Furdyna, J. Appl. Phys. **55**, 2310 (1984).

[18]A. Wittlin, R. Triboulet, and R. R. Galazka, J. Cryst. Growth **72**, 380 (1985).

[19]Y. Shapira, S. Foner, D. H. Ridgley, K. Dwight, and A. Wold, Phys. Rev. B **30**, 4021 (1984).

[20]A. Abragam and B. Bleaney, *Electron Paramagnetic Resonance of Transition Ions* (Claredon, Oxford, 1970), p. 92.

[21]Z. Wilamowski (unpublished).

[22]D. U. Bartholomew, E. K. Suh, S. Rodriguez, A. K. Ramdas, and R. L. Aggarwal, Solid State Commun. **62**, 235 (1987).

[23]E. A. Harris, J. Phys. C **5**, 338 (1972).

[24]E. D. Issacs, D. Heiman, P. Becla, Y. Shapira, R. Kersaw, K. Dwight, and A. Wold, Phys. Rev. B **38**, 8412 (1988).

[25]L. C. Brunel and M. Grynberg (private communication).

[26]A. Wittlin, Ph.D. thesis, Polish Academy of Sciences, 1982 (unpublished).

[27]J. H. Van Vleck, Phys. Rev. **74**, 1168 (1948).

[28]C. Kittel and E. Abrahams, Phys. Rev. **90**, 238 (1953).

[29]P. W. Anderson, J. Phys. Soc. Jpn. **9**, 316 (1954).

[30]I. Svare and G. Seidel, Phys. Rev. **134**, A172 (1964).

[31]B. E. Larson and H. Ehrenreich, Phys. Rev. B **39**, 1747 (1989).

[32]J. Owen and E. A. Harris, in *Electron Paramagnetic Resonances,* edited by S. Geschwind (Plenum, New York, 1972), p. 427.

[33]A. Abragam and B. Bleaney, *Electron Paramagnetic Resonance of Transition Ions* (Claredon, Oxford, 1970), p. 531.

[34]According to Fig. 6 the first level crossing ($S=0$, $S=1$, $M=-1$) should be at $B=J/g\mu$ ($\simeq 9$ T), and the second crossing ($S=1$, $M=-1$, $S=2$ $M=-2$) at the double field. Larson *et al.* (Ref. 10), however, found both crossings at slightly lower positions, which they ascribed to an additional molecular mean field caused by NNN and NNNN exchange terms. Therefore, it is difficult to obtain the exact value of J from the position of the level crossing as deduced from magnetization experiments.

[35]This transformation of coordinates is similar to the one presented in Ref. 20, p. 157 for the simplified case of axial symmetry ($E_s=0$).

[36]J. E. Gulley and V. Jaccarino, Phys. Rev. B **6**, 58 (1972).

[37]D. Scalbert, J. Cernogora, and C. Benoit a la Guillaume, *Proceedings of the 19th International Conference on the Physics of Semiconductors,* edited by W. Zawadzki (Polish Academy of Sciences, Warsaw, 1988), p. 1547.

[38]D. Scalbert, J. Cernogora, and C. Benoit a la Guillaume, Solid State Commun. **66**, 571 (1988).

[39]M. Blume and R. Orbach, Phys. Rev. **127**, 1587 (1962).

[40]N. Bloembergen, S. Shapiro, P. S. Pershan, and J. O. Artman, Phys. Rev. **114**, 445 (1959).

[41]R. B. Griffiths, Phys. Rev. **124**, 1023 (1961).